

# Controlled mechanochemical synthesis and properties of a selected perovskite-type electroceramics

PIOTR DULIAN<sup>1</sup>, WOJCIECH BĄK<sup>2</sup>, KRYSZYNA WIECZOREK-CIUROWA<sup>1\*</sup>, CZESŁAW KAJTOCH<sup>2</sup>

<sup>1</sup>Cracow University of Technology, Faculty of Chemical Engineering and Technology,  
24, Warszawska Str., 31-155 Cracow, Poland

<sup>2</sup>Pedagogical University, Institute of Physics, 2, Podchorążych Str., 30-084 Cracow, Poland

This paper presents mechanochemical synthesis as an alternative to the traditional high-temperature synthesis of advanced electrotechnical ceramic materials with a perovskite-type structure. The reaction conditions for high-energy ball milling, e.g. reaction environment, energy of milling and additives to BaTiO<sub>3</sub> such as metallic iron or zirconia from the exfoliation of the milling vessel and grinding media are discussed.

Keywords: *mechanochemistry; high-energy ball milling; perovskites; ferroelectric ceramics; barium titanate*

© Wrocław University of Technology.

## 1. Introduction

Mechanochemistry is a branch of solid-state chemistry that focuses on changing chemical and physicochemical properties of materials through the application of mechanical energy. While it is a relatively new area of science, mechanochemistry has its roots in prehistory, when mankind first realized that friction could be used to start fires. Since then, a mechanical approach has been used in modern technology and material engineering. Mechanochemical treatment has been used as an alternative method of synthesizing functional materials such as intermetallic compounds, composites, catalysts, sorbents and a wide range of ceramics. In high-energy ball milling, mechanical energy is added to the material and stored in the crystal lattice. This process is driven by structural changes such as the creation of defects and dislocations, loss of crystallinity, and thorough comminution of a material into nanosized powders. High-energy ball milling processes are carried out at ambient temperature, while the same syntheses using traditional solid-state reaction conditions demand high temperatures, occasionally

above 1300 K. Often, mechanically-synthesized materials display unique chemical properties compared to their conventionally-synthesized counterparts. It is also possible to form materials which cannot be made another way, e.g. oversaturated solid solutions.

Mechanochemistry is an example of *green chemistry*. These syntheses are simple one-pot processes, do not generate by-products, do not require organic solvents, and use mainly environmentally-innocuous inorganic reagents such as oxides or metals [1–14].

Such methods are useful for the manufacture of electrotechnical materials. The worldwide growth in the generation of electricity has stimulated the discovery of materials with high electrical conductivity and capacitance. Ceramics are of special interest for these applications.

Ceramics contain particularly strong bonds what results in a stable crystal structure. As such, the properties of these types of materials are exceptionally resistant to changes caused by the surrounding environment: they do not corrode or burn as metals or polymers. Further, a large diversity of crystal structures is readily accessible, as the ions which serve as structural elements can be easily exchanged for others. This provides practically limit-

\*E-mail: kwc@pk.edu.pl

less opportunities to tailor the electrical and magnetic properties of ceramic materials.

To perovskites, the best known example of which is barium titanate, careful attention must be paid. The wide range of ferroelectric properties displayed by  $\text{BaTiO}_3$  is well-understood owing to wide use of this material in electrotechnical applications [15–18]. By changing the grain morphology and chemical composition of  $\text{BaTiO}_3$ , it is possible to modify its electrical properties and thereby its applications [19–25].

Manufacturing these materials on an industrial scale traditionally requires a high-temperature method, which involves a lengthy heating of barium carbonate and titanium oxide at approximately 1620 K [26–29]. Not only this method is time and energy consuming, it is also incapable of producing fine crystals of  $\text{BaTiO}_3$ , which results in inferior material performance.

Other known methods of  $\text{BaTiO}_3$  synthesis include sol-gel [30], hydrothermal [31, 33] and coprecipitation processes [34]. While these methods allow good control over grain morphology, they are not widely used in industry owing to their complexity, and their need for expensive equipment, solvents, and organometallic reagents.

Kong et al. [35] and other authors [36–41] have used high-energy ball milling to activate substrates used to obtain barium titanate. This activation allowed the product to be realized at a lower temperature (ca. 1100 – 1200 K) and in a shorter span of time than in conventional methods.

On account of its advantages, mechanochemical synthesis of perovskites is the subject of intensive study. Particular attention should be paid to reaction environments and conditions, because the resulting properties of the materials depend on them. Also important is the role played by impurities introduced by the exfoliation of the walls of the reaction vessel and balls, which determines the properties of obtained electrotechnical ceramics.

The aim of the current work is to demonstrate mechanochemical synthesis as a method of fabricating advanced electro-ceramic material i.e. barium titanate. In this article, we discuss the influence of various reaction conditions and environments on the formation of  $\text{BaTiO}_3$ , and also elucidate the ef-

fect of contamination by metallic iron and zirconia on the electrical properties of the material.

## 2. Experimental

### 2.1. Synthesis materials

All materials used were oxides: BaO (Sigma Aldrich, 90 % M = 153.33 g/mol),  $\text{TiO}_2$  (Evonik Degussa P25 GmbH, 98.0 %, M = 79.90 g/mol). As the reaction vessels and balls were made of steel or  $\text{ZrO}_2$ , therefore metallic iron or zirconia were present also in final products.

### 2.2. Synthesis equipment and procedures

A stoichiometric ratio of oxides to  $\text{BaTiO}_3$  was mixed by hand in an agate mortar in order to obtain a homogenous mixture. This mixture was then subjected to mechanochemical treatment in two different high-energy planetary ball-mills:

a) *Activator 2S* (Novosibirsk Corp., Russia); milling was conducted at room temperature and in either air or in a solvent such as ethanol or water. A 250 ml reaction vessel was used, along with Cr–Ni steel ball-bearings 10 mm in diameter. The vessel was rotated at 1100 rpm for 1.5 hours, with a ball-to-powder weight ratio (BPR) of 40:1. This sample is designated as  $\text{BaTiO}_3/\text{Fe}$ .

b) *Pulverisette 6* (Fritsch GmbH, Germany); milling was also carried out at room temperature in air. A 250 ml reaction vessel was used along with  $\text{ZrO}_2$  ball-bearings 10 mm in diameter. The vessel was rotated at 550 rpm for 5 hours with a BPR of 20:1. This sample is designated as  $\text{BaTiO}_3/\text{Zr}$ .

### 2.3. High-temperature synthesis

Barium titanate was also synthesized using a high-temperature method as a control [29]. A stoichiometric mixture of oxides was formed into a tablet and heated for 4 hours at 1373 K in a Nabertherm HTC 03/15 laboratory furnace. This procedure was repeated three times. This sample is designated as  $\text{BaTiO}_3/\text{T}$ .

## 2.4. Characterization of as-synthesized materials

The as-synthesized materials were analyzed via powder X-ray diffraction with a  $\text{CuK}\alpha$  source on an X'Pert Philips instrument, within  $2\theta = 10^\circ - 90^\circ$  at a step size of  $0.01^\circ$ . Identification of the material was accomplished by consulting a JCPDS table.

Grain-size distribution was determined using a 22 MicroTec laser-diffraction apparatus (Fritsch GmbH).

The surface area of the materials was determined using BET (Brunauer, Emmet and Teller) physical adsorption isotherms. Measurements were taken using an Accelerated Surface Area and Porosimetry Analyzer (ASAP) 2020 from Micrometrics.

To determine the elemental composition of the products, particularly the amount of iron and zirconium that typically contaminate mechanochemically-treated samples, X-ray fluorescent spectroscopy (XRF) was used. XRF measurements were performed on a Bruker S4 Explorer.

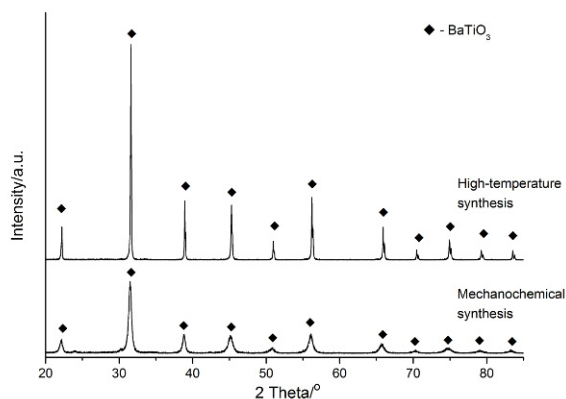


Fig. 1. Comparison of X-ray powder patterns of BaO and  $\text{TiO}_2$  mixture after high-temperature and mechanochemical syntheses (*Activator-2S* mill, rpm = 1100, BPR = 40:1).

For the purposes of testing the material electrical properties, a small sample was taken and pressed into a disc-pellet 7 mm in diameter and 2.5 mm thick, which was then heated in a Nabertherm HTC 03/15 laboratory furnace for 1 hour at 1373 K and painted with silver electrodes.

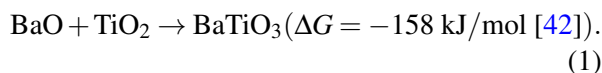
Dielectric spectroscopy measurements were conducted at a frequency between 20 Hz and 1 MHz, using an LCR Agilent 4284A instrument with QUATRO KRIO 4.0 temperature and WIN-Data 5.62 software (Novocontrol). All trials were carried out under nitrogen atmosphere. Measurements were performed between 173 K and 473 K, in 5 K increments. Amplitude of measuring voltage was 1 V.

## 3. Results and discussion

### 3.1. Mechanochemical synthesis of barium titanate

#### 3.1.1. The effects of mill vessel and ball bearing composition (steel, zirconia) on the dynamics of $\text{BaTiO}_3$ synthesis.

The synthesis of barium titanate proceeds according to reaction



(a) The results of  $\text{BaTiO}_3$  synthesis in the *Activator-2S* mill are illustrated in Fig. 1.

The formation of crystalline  $\text{BaTiO}_3$  can already be observed after 10 minutes of milling. A complete transformation into product is completed in 1.5 hours. Based on the broad, low-intensity primary peak of barium titanate, it is possible to conclude that the compound displays a small grain size, a low degree of crystallinity or a large number of crystal defects. The grain-size distribution of the products as shown in Fig. 2 appears to preclude the presence of small particles, as the majority of grains are approximately 10  $\mu\text{m}$  in diameter. However, it is worth remembering that mechanochemically-processed powders tend to form agglomerates, which may lead to errors in the interpretation of grain-size results. SEM photomicrographs (Fig. 3) provide convincing evidence in support of this conclusion, as they clearly show agglomerates across a large area of the sample. SEM observations demonstrate that the crystals are in fact on the order of 100 – 500 nm in size.

(b) The use of a lower-energy ball mill (*Pulverisette 6*) extends the reaction time required to ob-

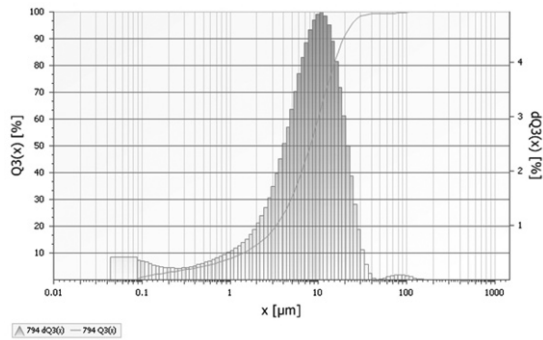


Fig. 2. Grain-size distribution of mechanochemically-synthesized BaTiO<sub>3</sub> (*Activator-2S*, 1100 rpm, BPR = 40:1).

tain single-phase BaTiO<sub>3</sub> to 5 hours. A prolonged mechanochemical treatment results in a larger BET surface area (Table 1).

Table 1. Comparison of BET specific surface areas.

Sample name	Surface area, BET [m <sup>2</sup> /g]	Pore volume [cm <sup>3</sup> /g]	Pore size [Å]
BaTiO <sub>3</sub> /Fe	7.159	0.021	110.985
BaTiO <sub>3</sub> /Zr	25.275	0.054	88.913
BaTiO <sub>3</sub> /T	0.24	n.d.	n.d.

n.d. – not determined

The abrasion of the reaction vessel and balls may contaminate the sample during high-energy milling. Powder X-ray diffraction did not indicate the presence of either iron or zirconia in the samples which evinces the small amount of both. It is also possible that these impurities were interstitially incorporated into the structure of BaTiO<sub>3</sub>, but the exact position and phase of the impurities is unknown at this time. The exact amounts of these impurities were found using XRF measurements, and the results are shown in Table 2.

Despite the fact that the samples milled with ZrO<sub>2</sub> were treated three times longer than those milled with steel, the amount of zirconium and iron in the resulting samples is comparable. A lower mill rotation speed, different hardness values and the nature of chemical bonds in the reaction vessel material likely causes differences in the way that the ball bearings abrade.

Table 2. Chemical composition of mechanically-synthesized BaTiO<sub>3</sub> powders.

Sample name	Metal wt. %	Relative uncertainty, %	
BaTiO <sub>3</sub> /Fe	Ba	62.03	0.34
	Ti	18.54	0.32
	Fe	1.23	0.11
BaTiO <sub>3</sub> /Zr	Ba	61.82	0.32
	Ti	17.12	0.34
	Zr	1.84	0.30

### 3.1.2. The influence of reaction environment (ethanol, water) on the synthesis of BaTiO<sub>3</sub>

When milling is conducted in water or ethanol, barium titanate is not formed even after 1.5 hours of high-energy milling in the *Activator-2S* mill. However, milling activates the substrates which on further heat treatment, can be transformed into BaTiO<sub>3</sub> at a lower temperature than in conventional high-temperature processes, using heating at 1070 K, (Fig. 4).

### 3.1.3. Comparing the morphologies of the BaTiO<sub>3</sub> powders obtained via mechanochemical and high-temperature methods

The mechanochemically obtained powders displayed different grain morphologies than those made using the conventional high-temperature method. The powder XRD diffraction pattern of the thermally-synthesized material is shown in Fig. 1.

BaTiO<sub>3</sub> synthesized using the high-temperature method had tetragonal symmetry at room temperature, in contrast to that obtained mechanochemically, which was cubic. The high degree of comminution and the large number of defects caused by high-energy ball milling limits long-range order in the crystallographic structure, and this prevents phase transitions. Calcination of the powder for 1 hour at 1373 K eliminates this problem.

Barium titanate, BaTiO<sub>3</sub>/T has a much smaller surface area and larger-diameter grains than the BaTiO<sub>3</sub>/Fe and BaTiO<sub>3</sub>/Zr samples (see Table 1) (Fig. 5). After sintering at high temperature, it was

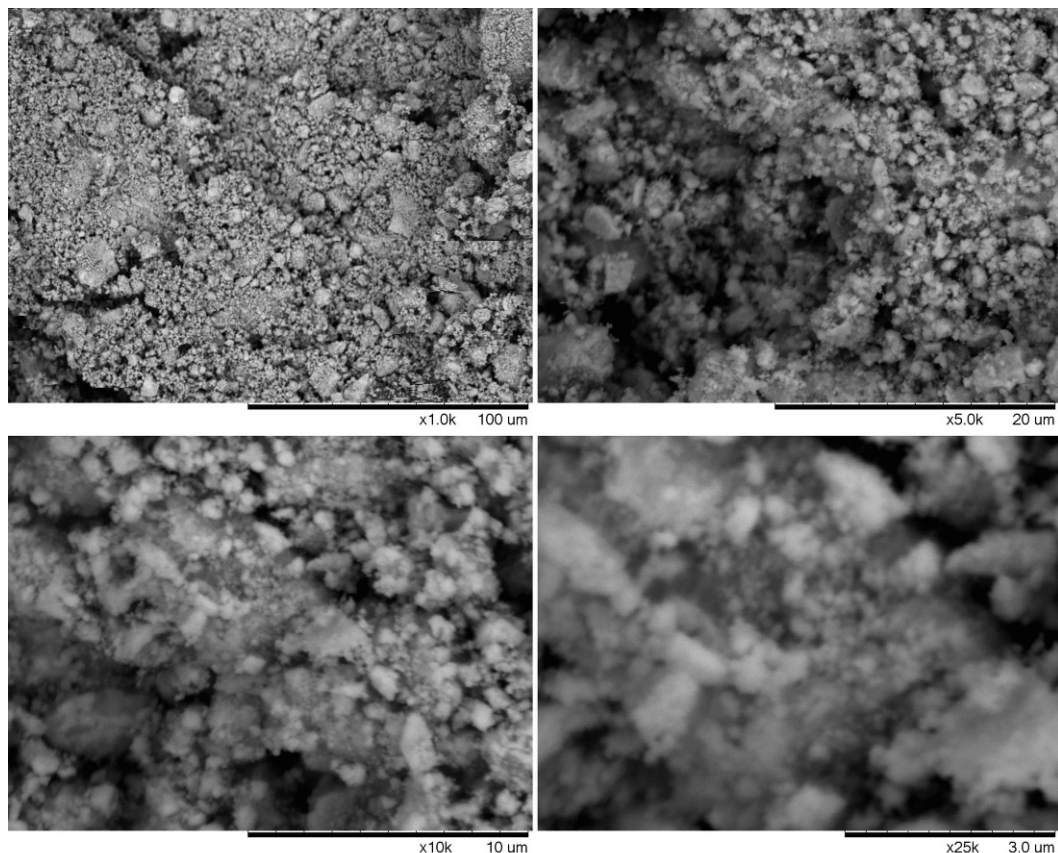


Fig. 3. SEM photomicrographs of as-synthesized BaTiO<sub>3</sub> (*Activator-2S*, 1100 rpm, BPR = 40:1).

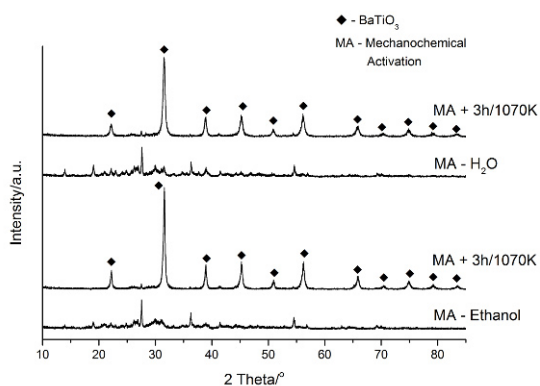


Fig. 4. Powder X-ray diffraction pattern of BaO and TiO<sub>2</sub> substrates subjected to 1.5 hours of mechanical activation (*Activator-2S*, 1100 rpm, BPR = 40:1) in water and ethanol and after 3 hours of heating at 1070 K.

impossible to measure the pore size and pore volume of BaTiO<sub>3</sub>/T.

### 3.2. Electrical properties of as-synthesized barium titanate

Electrical properties of as-synthesized BaTiO<sub>3</sub> were measured as temperature-dependences of the real ( $\epsilon'$ ) and imaginary ( $\epsilon''$ ) components of complex electrical permittivity, and the inverse of the real component of permittivity ( $1/\epsilon'$ ). These properties were determined at chosen frequencies of the electric field (1 kHz and 1 MHz).

Fig. 6 shows the results of the real part of the electrical permittivity for barium titanate synthesized mechanochemically with additional metallic iron (BaTiO<sub>3</sub>/Fe) and ZrO<sub>2</sub> (BaTiO<sub>3</sub>/Zr) (see Table 2), as well as the material synthesized via the high-temperature method (BaTiO<sub>3</sub>/T).

In the case of BaTiO<sub>3</sub>/T, the temperature at which  $\epsilon'$  is highest represents the paraelectric-ferroelectric (PE-FE) phase transition. At all frequencies of the electric field, a classical, sharp tran-

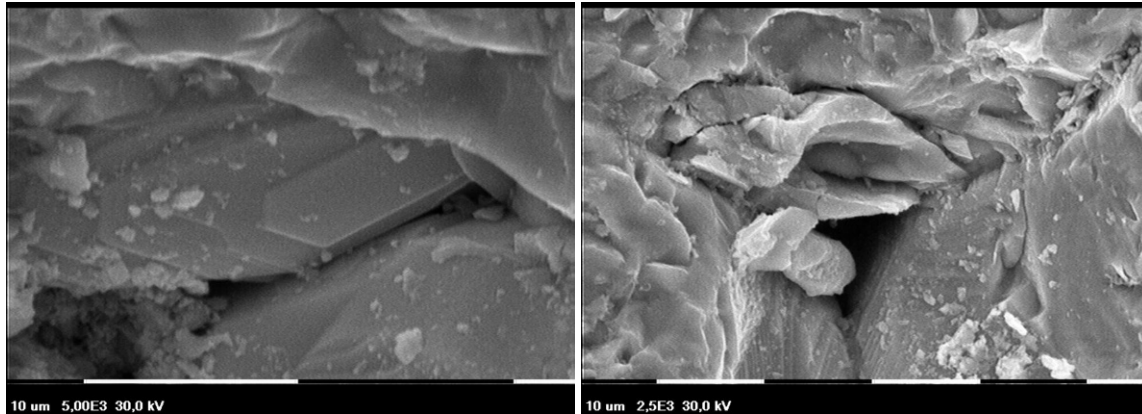


Fig. 5. SEM photomicrographs of BaTiO<sub>3</sub> powders (BaTiO<sub>3</sub>/T) obtained by high-temperature solid-state synthesis.

sition can be seen at 403 K, which corresponds to a structural shift between cubic and tetragonal phases. At 288 K there is another maximum, however its value is around four times smaller than the transition at 403 K. The observed temperature of this phase transition for BaTiO<sub>3</sub> varies from the literature value by 5 – 20 K [22–24]. It is possible to surmise that transition at 288 K corresponds to a change from a tetragonal structure to an orthorhombic one.

For BaTiO<sub>3</sub>/Zr ceramics, the PE-FE transition occurs at 368 K. This transition is found to be diffused, and the frequency of the electrical field somewhat changes the behavior of the material. A further lowering of the temperature causes greater peak diffusing compared to that observed in “clean” BaTiO<sub>3</sub>. No maximum is observed at 288 K.

The BaTiO<sub>3</sub>/Fe product has a characteristically-diffused peak at the PE-FE transition, the most diffused of any of the samples tested. The observed maximum of  $\epsilon'$  approaches a value of 3000 at a temperature of 303 K, nearly 100 K lower than the same transition in BaTiO<sub>3</sub>/T. Measurements at different frequencies of electrical field show that this material does not have the properties of a relaxor.

It is possible to postulate that the diffused character of the phase transition in BaTiO<sub>3</sub>/Zr and BaTiO<sub>3</sub>/Fe ceramics is caused by the substitutions of ions of a number of different charges into the cationic sub-lattice, but further testing is required.

In Fig. 7, the imaginary part of the temperature-dependent electrical permittivity ( $\epsilon''$ ) in an electrical field with frequencies of 1 kHz and 1 MHz is shown. The energy loss of the electric field represented by imaginary part of electrical permittivity ( $\epsilon''$ ) is associated with a structural phase change. The temperature at which  $\epsilon''(T)$  has a maximum correlates with the temperature at which  $\epsilon'(T)$  also has its maximum (Fig. 6). Above 303 K (the PE-FE transition temperature that was noted above), the BaTiO<sub>3</sub>/Fe sample inflicts a greater energy loss on the electric field than the BaTiO<sub>3</sub>/T and BaTiO<sub>3</sub>/Zr samples do. This temperature dependence of  $\epsilon''(T)$  indicates the dominant role of the electric field energy loss on determining the direct-current conductivity of the material.

The  $1/\epsilon'(T)$  graphs for the paraelectric phases of BaTiO<sub>3</sub>/T ( $T > 403$  K), BaTiO<sub>3</sub>/Zr ( $T > 368$  K) and BaTiO<sub>3</sub>/Fe ( $T > 303$  K) show the rightness of the Curie-Weiss law to these kinds of materials. The Curie-Weiss equation is shown below:

$$\epsilon = \frac{C}{T - T_0} \quad (2)$$

where  $C$  is the Curie-Weiss constant and  $T_0$  is the Curie-Weiss temperature.

The  $C$  and  $T_0$  constants for the measuring field frequency of 1 kHz and for the BaTiO<sub>3</sub>/T sample were appointed based on a linear regression procedure (Fig. 8). Their values are  $1.12 \cdot 10^5$  K and 390 K, respectively. Verifying the validity of the

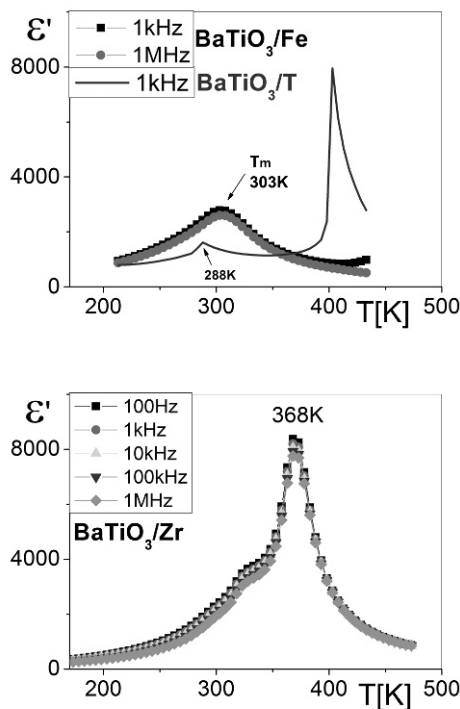


Fig. 6. The temperature dependence of real part of dielectric permittivity ( $\epsilon'$ ) for  $\text{BaTiO}_3/\text{T}$ ,  $\text{BaTiO}_3/\text{Fe}$  and  $\text{BaTiO}_3/\text{Zr}$  samples.

Curie-Weiss law for  $\text{BaTiO}_3/\text{Zr}$  sample one can see a little diversity of constants  $C$  and  $T_0$  depending on frequency. The values of  $C$  constant  $8.75 \cdot 10^4$  K and  $T_0$  temperature of 371 K were obtained from the linear fit at the frequency of 1 MHz, and for the frequency of 1 kHz these constants are  $8.77 \cdot 10^4$  K and 372 K, respectively. For the sample  $\text{BaTiO}_3/\text{Fe}$ , these constants values are  $7.08 \cdot 10^4$  K and 297 K (1 MHz) and  $8.34 \cdot 10^4$  K and 290 K (1 kHz), respectively, and show the greatest differences.

For  $\text{BaTiO}_3/\text{T}$  and  $\text{BaTiO}_3/\text{Zr}$  samples the degree of diffusion of PE-FE phase transition is small and corresponds to the sharp phase transition (first-order) whereas  $\text{BaTiO}_3/\text{Fe}$  sample shows diffuse PE-FE phase transition.

#### 4. Final remarks

1) Synthesis of  $\text{BaTiO}_3$  using high-energy ball milling demonstrated the possibility of manufacturing advanced electrotechnical ceramic materials,

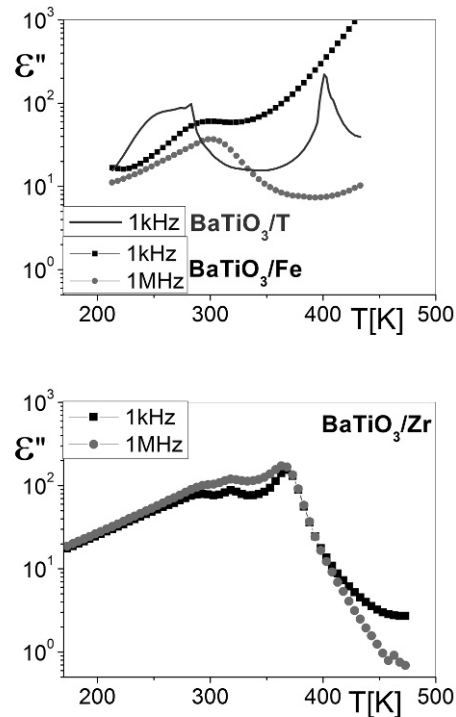


Fig. 7. The temperature dependence of imaginary components of the dielectric permittivity for  $\text{BaTiO}_3/\text{T}$ ,  $\text{BaTiO}_3/\text{Fe}$  and  $\text{BaTiO}_3/\text{Zr}$  samples.

using conditions that are in accord with the principles of *green chemistry*.

2) The properties of barium titanate and the two methods of obtaining it are shown in Table 3. It is clear that the material obtained via mechanochemical methods has better properties than those obtained via traditional high-temperature synthesis. The ferroelectric phase transitions occur at a wider range of temperatures, and the materials also display high dielectric permittivity ( $\epsilon$ ).

3) Impurities in the product such as metallic iron or zirconia that are exfoliated from the reaction vessel and grinding media are difficult to remove. However, it is clear that this can be advantageous, and used to control the electrical properties of the obtained material.

#### Acknowledgements

This study was supported by the Polish Ministry of Science and Higher Education, projects CUT C-1/KWC/DS/2012-2013 and UMO-2012/05/N/ST8/03764. The authors wish to thank Mr. Mark Kozłowski, Fulbright Fellow at CUT, for language verification of the article.

Table 3. Synthesis conditions and characteristics of BaTiO<sub>3</sub> products.

Method of synthesis (sample)	Conditions of synthesis	Specific surface area	Paraelectric-ferroelectric phase transition
High-temperature synthesis (BaTiO <sub>3</sub> /T)	12 h at 1373 K	Small value (large, sintered grains)	Sharp at 403 K
Mechanochemical syntheses (BaTiO <sub>3</sub> /Fe); (BaTiO <sub>3</sub> /Zr)	1.5 – 5 h at ambient temperature	High comminution (with a tendency to agglomerate)	Diffused (BaTiO <sub>3</sub> /Zr – at 368 K, BaTiO <sub>3</sub> /Fe – at 303 K)

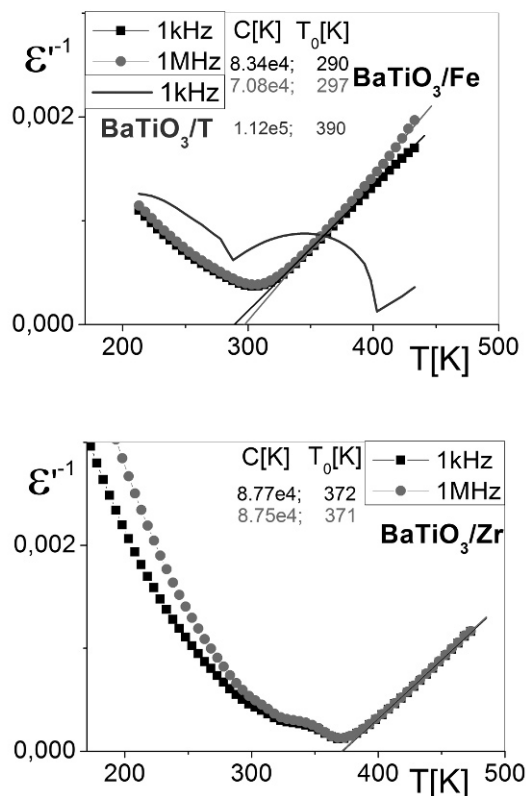


Fig. 8. The inverse of the real part of complex dielectric permittivity as a function of temperature at chosen frequencies for BaTiO<sub>3</sub>/T, BaTiO<sub>3</sub>/Fe and BaTiO<sub>3</sub>/Zr samples.

## References

- [1] BOLDYREV V.V., TKÁČOVÁ K., *J. Mater. Synth. Process.*, 8 (3–4) (2000), 121.
- [2] GILMAN J.J., *Science*, 39 (1996), 65.
- [3] SURYANARAYANA C., *Prog. Mater. Sci.*, 46 (2001), 1.
- [4] WIECZOREK-CIUROWA K., *Mechanochemical Synthesis of Metallic-Ceramic Composite Powders*, in: M. Sopicka-Lizer (Eds.), *High-Energy Ball Milling: Mechanochemical Processing of Nanopowders*, Woodhead Publishing Ltd., 2010, p. 193.
- [5] TAKACS L., *Prog. Mater. Sci.*, 47 (2002), 355.
- [6] AVVAKUMOV E., *Soft Mechanochemical Synthesis: A Basis for New Chemical Technologies*, Kluwer Academic Publishers, Boston, 2001.
- [7] WIECZOREK-CIUROWA K., RAKOCZY J., BŁOŃSKA-TABERO A., FILIPEK E., NIZIOŁJ., DULIAN P., *Catal. Today*, 176 (2011), 314.
- [8] ZHANG W., LU L., CHENG Y., XU N., PAN L., LIN Q., WANG Y., *Green Chem.*, 13 (2011), 2701.
- [9] WIECZOREK-CIUROWA K., DULIAN P., NOSAL A., DOMAGAŁA J., *J. Therm. Anal. Calorim.*, 101 (2010), 471.
- [10] WIECZOREK-CIUROWA K., DULIAN P., BAK W., KAJTOCH C., *Przem. Chem.*, 90 (2011), 1400. (in Polish).
- [11] ZHANG Q., SAITO F., *Adv. Powder Technol.*, 23 (2012), 523.
- [12] WIECZOREK-CIUROWA K., GAMRAT K., *J. Therm. Anal. Calorim.*, 88 (2007), 213.
- [13] GARAY A.L., PICHON A., JAMES S.L., *Cryst. Eng. Comm.*, 8 (2007), 846.
- [14] CARLIER L., BARON M., CHAMAYOU A., COURRAZE G., *Tetrahedron Lett.*, 52 (2011), 4686.
- [15] JOHNSON C.J., *Appl. Phys. Lett.*, 7 (1965), 221.
- [16] GEORGE C.N. et al., *J. Mater. Charact.*, 60 (2009), 322.
- [17] BUSCAGLIA V. et al., *Powder Technol.*, 148 (2004), 24.
- [18] HENNINGS D., *Int. J. Hig Technol. Ceram.*, 3 (1987), 91.
- [19] VÖLTZKE D., ABICHT H.-P., *J. Mater. Sci.*, 30 (1995), 4896.
- [20] LIN T.-F., LIN J.-L., HU C.-T., LIN I.-N., *J. Mater. Sci.*, 26 (1991), 491.
- [21] KUMAR P., SINGH S., SPAH M., JUNEJA J.K., PRAKASH C., RAINA K.K., *J. Alloys Compd.*, 489 (2010), 59.
- [22] NATH A.K., MEDHI N., *Mater. Lett.*, 73 (2012), 75.

- [23] KINOSHITA K., YAMAJI A., *J. Appl. Phys.*, 47 (1976), 371.
- [24] BUSCAGLIA V. et al., *J. Eur. Ceram. Soc.*, 26 (2006), 2889.
- [25] FREY M.H., PAYNE D.A., *Phys. Rev. B: Condens. Matter Mater. Phys.*, 54 (1996), 3158.
- [26] NIEPCE J.C., THOMAS G., *Solid State Ionics*, 43 (1990), 69.
- [27] BHALLA A.S., GUO R., ROY R., *Mater. Res. Innovations*, 4 (2000), 3.
- [28] JUNG W.S., KIM J.H., KIM H.T., YOON D.H., *Mater. Lett.*, 64 (2010), 170.
- [29] TSUZUKU K., COUZI M., *J. Mater. Sci.*, 47 (2012), 4481.
- [30] FREY M.H., PAYNE D.A., *Appl. Phys. Lett.*, 63 (1993), 2753.
- [31] LEI J.-X., LIU X.-L., CHEN J.-F., *Adv. Mater. Res.*, 11 – 12 (2006), 23.
- [32] TESTINO A., BUSCAGLIA V., BUSCAGLIA M.T., VIVIANI M., NANNI P., *Chem. Mater.*, 17 (2005), 5346.
- [33] XU H., GAO L., *Mater. Lett.*, 57 (2002), 490.
- [34] WU D.H., SHI X.Y., ZHANG H.J. S., *Yadian Yu Shengguang/Piezoelectric and Acoustooptics*, 31 (2009), 251.
- [35] KONG L.B., MA J., HUANG H., ZHANG R.F., QUE W.X., *J. Alloys Compd.*, 337 (2002), 226.
- [36] SUNDARARAJAN T., BALASIVANANDHA PRABU S., MANISHA VIDYAVATHY S., *Mater. Res. Bull.*, 47 (2012), 1448.
- [37] ZAZHIGALOV V.A., SIDORCHUK V.V., KHALAMEIDA S.V., KUZNETSOVA L.S., *Inorg. Mater.*, 44 (2008), 641.
- [38] GOMEZ-YAÑEZ C., BENITEZ C., BALMORIRAMIREZ H., *Ceram. Int.*, 26 (2000), 271.
- [39] ABE O., SUZUKI Y., *Mater. Sci. Forum*, 225 (part 1) (1996), 563.
- [40] STOJANOVIC B.D., SIMOES A.Z., PAIVA-SANTOS C.O., JOVALEKIC C., MITIC V.V., VARELA J.A., *J. Eur. Ceram. Soc.*, 25 (2005), 1985.
- [41] BRZOWSKI E., CASTRO M.S., *Thermochim. Acta*, 398 (2003), 123.
- [42] BARIN I., KNACKE O., KUBASCHEWSKI O., *Thermochemical Properties of Inorganic Substances*, Springer-Verlag, Berlin, 1977.

Received 2012-12-07  
Accepted 2013-05-31